

## PDF hosted at the Radboud Repository of the Radboud University Nijmegen

The following full text is a preprint version which may differ from the publisher's version.

For additional information about this publication click this link.

<http://hdl.handle.net/2066/72205>

Please be advised that this information was generated on 2019-11-19 and may be subject to change.

# Dual fermion approach to nonlocal correlations in the Hubbard model

A. N. Rubtsov,<sup>1</sup> M. I. Katsnelson,<sup>2</sup> and A. I. Lichtenstein<sup>3</sup>

<sup>1</sup>*Department of Physics, Moscow State University, 119992 Moscow, Russia*

<sup>2</sup>*Institute for Molecules and Materials, Radboud University, 6525 ED Nijmegen, The Netherlands*

<sup>3</sup>*Institute of Theoretical Physics, University of Hamburg, 20355 Hamburg, Germany*

A new diagrammatic technique is developed to describe nonlocal effects (e.g., pseudogap formation) in the Hubbard-like models. In contrast to cluster approaches, this method utilizes an exact transition to the dual set of variables, and it therefore becomes possible to treat the irreducible vertices of an effective *single-impurity* problem as small parameters. This provides a very efficient interpolation between weak-coupling (band) and atomic limits. The antiferromagnetic pseudogap formation in the Hubbard model is correctly reproduced by just the lowest-order diagrams.

PACS numbers: 71.10.Fd, 71.27.+a, 05.30.Fk

Lattice fermion models with a strong local interaction (Hubbard-like models [1]) are believed to catch the basic physics of various systems, such as high-temperature superconductors [2, 3], itinerant-electron magnets [4], Mott insulators [5], ultracold atoms in optical lattices [6], etc. Unfortunately, the analytical treatment of these problems is essentially restricted by the lack of explicit small parameters for the most physically interesting interactions. Direct numerical methods, such as exact diagonalization [7] or quantum Monte Carlo (QMC) [8, 9] are limited by the clusters being of a relatively small size, or face other obstacles such as the famous sign problem for QMC simulations at low temperature [10]. There is a very successful approximate way to treat these models via the framework of so-called dynamical mean-field theory (DMFT) [5], where the lattice many-body problem is replaced with an effective impurity model. This approach is essentially based on the assumption of a local (i.e. momentum-independent) fermionic self energy. Indeed, there are numerous interesting phenomena which are basically determined by *local* electron correlations, such as Kondo effect [11], Mott-Hubbard transitions [5] and local moment formation in itinerant-electron magnets [12]. At the same time, momentum dependence of the self energy is of crucial importance for Luttinger liquid formation in low-dimensional systems [3, 13], d-wave pairing in high- $T_c$  superconductors [2, 14, 15], and non-Fermi-liquid behavior due to van Hove singularities in two dimensions [16]. Recently a rather strong momentum dependence of the effective mass renormalization in photoemission spectra of iron was observed [17].

Currently, non-local many body effects in strongly correlated systems are mainly studied via the framework of various cluster generalizations of DMFT [14, 15, 18, 19]. Cluster methods do catch basic physics of d-wave pairing and antiferromagnetism in high- $T_c$  superconductors [14, 15], and the effects of intercite Coulomb interaction in various transition-metal oxides [20, 21, 22]. At the same time, however effects like Luttinger liquid formation or van Hove singularities can not be described in cluster approaches. In such cases the correlations are essentially

long-ranged and it is more natural to describe the correlations in momentum space. Recently attempts have been made to consider non local correlation effects in momentum space starting from DMFT as a zeroth-order approximation [23, 24]. This approach requires a solution of ladder-like integral equation for complete vertex  $\Gamma$  and the subsequent use of the Bethe-Salpeter equation to obtain Green's functions. The first step here exploits an irreducible vertex of the effective impurity problem  $\gamma^{(4)}$ , whereas the second step uses just the bare interaction parameter  $U$ . This second step makes the generalized DMFT approach mostly suitable to the weak-coupling regime [25].

In this Letter, we present a scheme which is accurate in both small- $U$  and large- $U$  limits and does not require numerically expensive solutions of any integral equations. A comparison of the results with lattice QMC simulations for the two-dimensional (2D) Hubbard model in the pseudogap regime demonstrates that the scheme is actually accurate even in the less-favorable case of intermediate  $U$ .

We proceed with 2D Hubbard model with the corresponding imaginary-time action

$$S[c, c^*] = \sum_{\omega k \sigma} (\epsilon_k - \mu - i\omega) c_{\omega k \sigma}^* c_{\omega k \sigma} + U \sum_i \int_0^\beta n_{i\uparrow\tau} n_{i\downarrow\tau} d\tau. \quad (1)$$

Here  $\beta$  and  $\mu$  are the inverse temperature and chemical potential, respectively,  $\omega = (2j+1)\pi/\beta$ ,  $j = 0, \pm 1, \dots$  are the Matsubara frequencies,  $\sigma = \uparrow, \downarrow$  is the spin projection. The bare dispersion law is  $\epsilon_k = -2t(\cos k_x + \cos k_y)$ ,  $c^*$ ,  $c$  are the Grassmannian variables,  $n_{i\sigma\tau} = c_{i\sigma\tau}^* c_{i\sigma\tau}$ , where the indices  $i$  and  $k$  label sites and quasi-momenta.

In the spirit of DMFT, we introduce a single-site reference system (an effective impurity model) with the action

$$S_{imp} = \sum_{\omega, \sigma} (\Delta_\omega - \mu - i\omega) c_{\omega, \sigma}^* c_{\omega, \sigma} + U \int_0^\beta n_{\uparrow\tau} n_{\downarrow\tau} d\tau \quad (2)$$

where  $\Delta_\omega$  is as an yet undefined hybridization function describing the interaction of the effective impurity with

a bath. We suppose that all properties of the impurity problem are known, so that its single-particle Green's function  $g_\omega$  is known, and the irreducible vertex parts  $\gamma^{(4)}, \gamma^6$ , etc. Our goal is to express the Green's function  $G_{\omega k}$  and vertices  $\Gamma$  of the lattice problem in Eq.(1) via these quantities.

Since  $\Delta$  is independent of  $k$ , the action (1) can be represented in the form

$$S[c, c^*] = \sum_i S_{imp}[c_i, c_i^*] - \sum_{\omega k \sigma} (\Delta_\omega - \epsilon_k) c_{\omega k \sigma}^* c_{\omega k \sigma}. \quad (3)$$

We utilize a dual transformation to the set of new Grassmannian variables  $f, f^*$ . The following identity

$$e^{A^2 c_{\omega k \sigma}^* c_{\omega k \sigma}} = B^{-2} \int e^{-AB(c_{\omega k \sigma}^* f_{\omega k \sigma} + f_{\omega k \sigma}^* c_{\omega k \sigma}) - B^2 f_{\omega k \sigma}^* f_{\omega k \sigma}} df_{\omega k \sigma}^* df_{\omega k \sigma}, \quad (4)$$

is valid for arbitrary complex numbers  $A$  and  $B$ . We chose  $A^2 = (\Delta_\omega - \epsilon_k)$  and  $B^2 = g_\omega^{-2}(\Delta_\omega - \epsilon_k)^{-1}$  for each set of indices  $\omega, k, \sigma$ .

With this identity, the partition function of the lattice problem  $Z = \int e^{-S[c, c^*]} \mathcal{D}c^* \mathcal{D}c$  can be presented in a form  $Z = Z_f \int \int e^{-S[c, c^*, f, f^*]} \mathcal{D}f^* \mathcal{D}f \mathcal{D}c^* \mathcal{D}c$ , where

$$S[c, c^*, f, f^*] = \sum_i S_{imp}[c_i, c_i^*] + \sum_{\omega k \sigma} [g_\omega^{-1}(f_{\omega k \sigma}^* c_{\omega k \sigma} + c_{\omega k \sigma}^* f_{\omega k \sigma}) + g_\omega^{-2}(\Delta_\omega - \epsilon_k)^{-1} f_{\omega k \sigma}^* f_{\omega k \sigma}] \quad (5)$$

and  $Z_f$  is a product  $\prod_{\omega k} g_\omega^2 (\Delta_\omega - \epsilon_k)$ .

As a next step, we establish an exact relation between the Green's function of the initial system  $G_{\tau-\tau', i-i'} = -\langle T c_{\tau i} c_{\tau' i'}^* \rangle$  and that of the dual system  $G_{\tau-\tau', i-i'}^{dual} = -\langle T f_{\tau i} f_{\tau' i'}^* \rangle$ . To this aim, we can replace  $\epsilon_k \rightarrow \epsilon_k + \delta\epsilon_{\omega k}$  with a differentiation of the partition function with respect to  $\delta\epsilon_{\omega k}$ . Since we have two expressions for the action (1) and (5), one obtains

$$G_{\omega, k} = g_\omega^{-2} (\Delta_\omega - \epsilon_k)^{-2} G_{\omega, k}^{dual} + (\Delta_\omega - \epsilon_k)^{-1}, \quad (6)$$

where the last term follows from the differentiation of  $Z_f$ .

The crucial point is that the integration over the initial variables  $c_i^*, c_i$  can be performed separately for each lattice site, since  $\sum_k (f_k^* c_k + c_k^* f_k) = \sum_i (f_i^* c_i + c_i^* f_i)$ . For a given site  $i$ , one should integrate out  $c_i^*, c_i$  from the action that equals  $S_{site}[c_i, c_i^*, f_i, f_i^*] = S_{imp}[c_i, c_i^*] + \sum_\omega g_\omega^{-1} (f_\omega^* c_\omega + c_\omega^* f_\omega)$ . We obtain

$$\int e^{-S_{site}} \mathcal{D}c_i^* \mathcal{D}c_i = Z_{imp} e^{-\sum_\omega g_\omega^{-1} f_{\omega i \sigma}^* f_{\omega i \sigma} - V[f_i, f_i^*]}, \quad (7)$$

where  $Z_{imp}$  is a partition function of the impurity problem (2). The Taylor series for  $V[f_i, f_i^*]$  in powers of  $f_i, f_i^*$  starts from  $-\gamma_{1234}^{(4)} f_1^* f_2^* f_3^* f_4$  (indices stand for a combination of  $\sigma$  and  $\omega$ , for example  $f_1^*$  means  $f_{\sigma_1, \omega_1}^*$ ). Further Taylor series terms yield similar combinations including  $\gamma^{(n)}$  of higher orders.

We arrive with an action  $S$  depending on the new variables  $f, f^*$  only:

$$S[f, f^*] = \sum_{\omega k \sigma} g_\omega^{-2} ((\Delta_\omega - \epsilon_k)^{-1} + g_\omega) f_{\omega k \sigma}^* f_{\omega k \sigma} + \sum_i V_i, \quad (8)$$

with  $V_i \equiv V[f_i^*, f_i]$ . In this dual action, the interaction terms remain localized in space, but are non-local in imaginary time, since, for example  $\gamma^{(4)}$  depends on the three independent Matsubara frequencies. To obtain the dual potential  $V$  for a practical calculation, one should solve then the impurity problem (2).

Finally a regular diagrammatic expansion in powers of  $V$  can be performed. We draw skeleton diagrams, so that the lines in diagrams are renormalized dual Green's function, whereas the vertices are  $\gamma^{(n)}$ . The rules of diagram construction are very similar to usual ones, but the six-leg and higher-order vertices appear because  $\gamma^{(6)}$  and higher terms are present in the series for  $V$ . Figure 1 shows several diagrams contributing dual self-energy  $\Sigma_{\omega, k}^{dual} = -[(\Delta_\omega - \epsilon_k)^{-1} g_\omega^{-2} + g_\omega^{-1} + (G_{\omega, k}^{dual})^{-1}]$ .

We use the skeleton-diagram expansion for the dual self-energy since it leads to the conserving theories, exactly like in conventional diagram technique [26, 27, 28]. The Baym criterion of a conservative theory is the existence of a functional of the Green function  $\Phi[G]$  such that  $\frac{\delta \Phi}{\delta G} = \Sigma$ . Here, the variation  $\delta G$  comes from the infinitesimal variation of the Gaussian part of the action,  $\delta(G^0)^{-1} c^* c$ . In our consideration, we consider also the infinitesimal variations of the dual potential  $\delta(G_{dual}^0)^{-1} c^* c$ . One can call an approximation dually  $\Phi$ -derivable, if there exists a functional  $\Phi^{dual}[G^{dual}]$  such as  $\frac{\delta \Phi^{dual}}{\delta G^{dual}} = \Sigma^{dual}$ , where the variation comes from  $\delta(G_{dual}^0)^{-1}$ . Now, it turns out that the theory is  $\Phi$ -derivable if it is dually  $\Phi$ -derivable. The proof uses the relation between functional  $\Phi$  and the partition function  $\ln Z = \Phi - \text{Tr} \Sigma G - \text{Tr} \ln(-G) + C$  (here  $C$  is an additive constant; see Ref.27, Eq.(47)). Since a similar relation takes place for  $\Phi^{dual}$  and  $\ln Z$  and since the partition

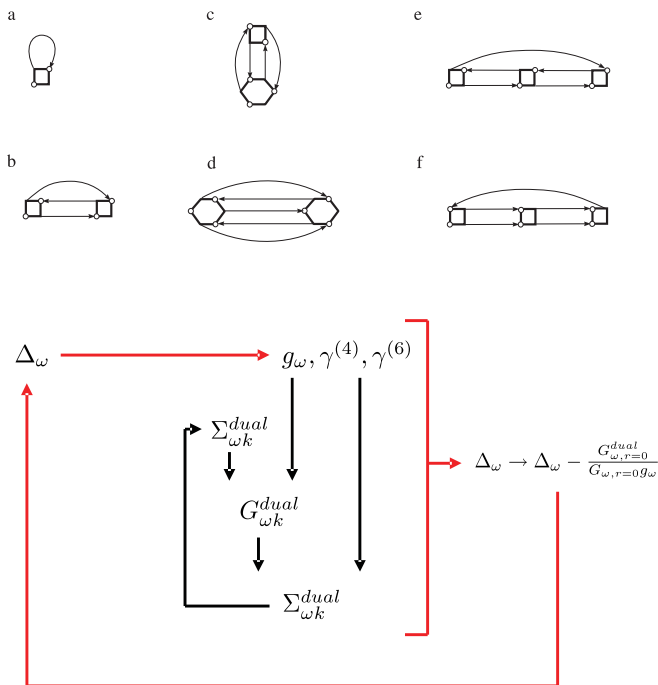


FIG. 1: (color online) Various diagrams for  $\Sigma^{dual}$  and the scheme of calculation. The calculation includes “big” and “small” loop, marked with red and black lines, respectively. The small loop is to determine the renormalized dual Green’s function  $G^{dual}$  in a self-consistent way, for given  $\Delta, g$ , and  $\gamma^{(n)}$ . The big loop is to determine  $\Delta$ . Only the big loop requires a solution of the impurity problem.

function is the same for the initial and dual variables, this gives a one-to-one correspondence between  $\Phi[G]$  and  $\Phi^{dual}[G^{dual}]$ . This is just a sketch; the detailed proof will be published elsewhere.

It is important to understand what can be a small parameter in the expansion in dual diagrams. Clearly, if  $U$  is small, then  $\gamma^{(4)} \propto U$ ,  $\gamma^{(6)} \propto U^2$  etc., and in the weak-correlated regime vertices in the diagrams will be small (Fig. 1), and higher-order vertices will be even smaller.

At this point we establish a condition for  $\Delta$ , which was so far an arbitrary quantity. We use a self-consistent condition

$$\sum_k G_{\omega,k}^{dual} = 0. \quad (9)$$

It means that the simple closed loops in diagrams vanish. In particular, this leads to the vanishing of the first-order “Hartree” corrections in the diagrammatic expansion. The diagram series of this kind has several important peculiarities. First of all, let us consider the zeroth-order approximation,  $\Sigma^{(dual)} = 0$ . In this case, the condition (9) becomes

$$\sum_k \frac{1}{g_\omega + (\Delta_\omega - \epsilon_k)^{-1}} = 0. \quad (10)$$

It is easy to show that this is exactly equivalent to the DMFT equation for the “hybridization function”  $\Delta_\omega$  [5]. It is known that DMFT behaves correctly near the atomic limit. In terms of the dual variables, one can observe that since  $\epsilon, \Delta \ll g^{-1}$  near the atomic limit, it follows from the condition (10) that  $G^{dual} \approx g_\omega^2 \epsilon_k \ll g_\omega$  in this case. It is easy to check that this argumentation is valid the scheme of an arbitrary diagrammatic order: the dispersion of  $G^{dual}$  is small near the atomic limit and therefore (9) means that lines in dual diagrams carry a small factor  $\epsilon g^{-1}$ . This ensures the fast convergence of new diagrammatic expansion in the strong-coupling limit.

As the most challenging test of our approximation scheme in the intermediate regime, we performed the calculation for the half-filled square-lattice Hubbard model, at sufficiently low temperature  $\beta^{-1} = |t|/5$ . The value of  $U$  was varied from small numbers to a bandwidth  $8|t|$ . The block scheme of our calculation is shown in Fig. 1. It has a good practical convergence: typically, about 10 iteration are enough to ensure convergence.

In order to obtain reference point for a further comparison with the results of our new approximation scheme, we performed a direct lattice QMC calculation with the continuous-time QMC code [30]. There are strong antiferromagnetic fluctuations in the system, although true antiferromagnetism is impossible at finite temperature in the 2D system with an isotropic order parameter [29]. Consequently, the increase of  $U$  results in a formation of an antiferromagnetic pseudogap.

It was also noticed that single-site DMFT calculation for this system shows no pseudogap in the density of states, although the data for local part of self-energy are reproduced quite well in DMFT. Thus we concluded that the formation of pseudogap is entirely related to the non-local part of  $\Sigma$ , neglected in DMFT.

We present the results of the dual-fermion calculation with only diagram (b) taken into account. All other diagrams are smaller both in the strong-coupling and weak-coupling regime, due to extra vertices or extra lines, respectively. Computational results are illustrated by Fig. 2. The upper panel shows an imaginary part of the self-energy. In the DMFT this quantity is momentum-independent. Our calculations show a very strong  $\mathbf{k}$ -dependence with a maximum near the Fermi surface. At relatively small value  $U = 1$  the peaks of  $\text{Im}\Sigma$  are located near the van Hove singularities (left picture), as it can be understood from the weak-coupling expansion. Contrary, for an antiferromagnetic system near the atomic limit,  $\text{Im}\Sigma_{k,\omega=0}$  would be a simple delta-function peaking at Fermi surface. For a pseudogap regime at finite  $\beta, U$ , the width of this peak is of course finite, but the altitude almost does not depend on the point at Fermi surface (right picture). The lower panel shows an effective renormalized dispersion law  $\epsilon_k + \text{Re}\Sigma_{k,\omega=0}$ . For the metallic regime, the renormalization is small. For an antiferromagnetic insulator, there would be a pole in  $\text{Re}\Sigma_{k,\omega=0}$  at the Fermi

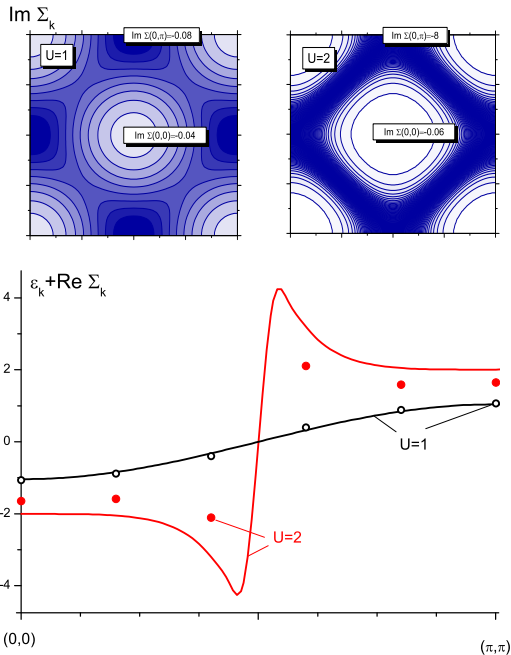


FIG. 2: (color online) Fermi-energy properties of the half-filled Hubbard model calculated with the leading dual diagram correction  $b$ . The calculations have been performed for the bandwidth  $8t = 2$  at  $\beta = 20$ , for different values of  $U$ . UPPER PANELS are contour plots for  $\text{Im}\Sigma_k$  at Fermi energy. At  $U = 1$ ,  $\text{Im}\Sigma$  peaks in the four van Hove points, whereas  $\text{Im}\Sigma(U = 1)$  is approximately constant in all points of the Fermi surface. Note also that the change from  $U = 1$  to  $U = 2$  leads to a  $10^2$  increase in  $\text{Im}\Sigma$ . LOWER PANEL shows a graph of the effective dispersion law,  $\epsilon_k + \text{Re}\Sigma_k$  at Fermi level, plotted along the  $(0,0) - (\pi,\pi)$  direction. The initial “cosine” dispersion law  $\epsilon_k$  is almost not renormalized at  $U = 1$ . Contrary, for  $U = 2$  the curve shows the antiferromagnetic properties. The result of direct QMC  $10 \times 10$  lattice simulation are shown with dots and confirm this picture.

surface. For the pseudogap regime, fluctuations virtually move this pole from the real-frequency axes, as the curve for  $U = 2$  shows.

Thus, our scheme continuously interpolate between the two very different regimes. It should be stressed that the quantities under study have very strong  $k$ -dependence and that it would be very difficult to obtain the result of this kind, for example, in cluster calculations. Whereas for the weak-coupling regime effective schemes to calculate nonlocal self-energy are known, such as FLEX [28] or parquet [16], to our knowledge, there is no alternative scheme yet for the strong coupling case.

To conclude, we have formulated an effective perturbation theory to calculate the momentum dependence of self energy starting with single-site DMFT or any local approximations. The vertices of the effective impurity

problem play the role of formal small parameters. Due to the transformation to dual fermionic variables, consideration of a few leading diagrams provides a quite satisfactory description of the nonlocal correlation effects in a broad range of parameters, up to the atomic limit. This scheme can be easily generalized to multiband case to be implemented into realistic electronic structure calculations for strongly correlated systems.

The work was supported by NWO project 047.016.005 and FOM (the Netherlands), DFG Grant No. SFB 668-A3 (Germany), and Leading scientific schools program and “Dynasty” foundation (Russia).

- 
- [1] J. Hubbard, Proc. Roy. Soc. (London), Ser. A **276**, 238 (1963).
  - [2] D. J. Scalapino, Phys. Rep. **251**, 1 (1994); J. Low Temp. Phys. **117**, 179 (1999).
  - [3] P. W. Anderson, *The Theory of Superconductivity in High- $T_c$  Cuprates* (Princeton Univ. Press, Princeton, 1997).
  - [4] T. Moriya, *Spin Fluctuations in Itinerant Electron Magnetism* (Springer, Berlin, 1985).
  - [5] A. Georges *et al*, Rev. Mod. Phys. **68**, 13 (1996).
  - [6] G. Modugno *et al*, Phys. Rev. A **68**, 011601(R) (2003); M. Köhl *et al*, Phys. Rev. Lett. **94**, 080403 (2005); J. K. Chin *et al*, Nature **443**, 961 (2006).
  - [7] E. Dagotto, Rev. Mod. Phys. **66**, 13 (1994).
  - [8] R. Blankenbecler *et al*, Phys. Rev. D **24**, 2278 (1981).
  - [9] J. E. Hirsch and R. M. Fye, Phys. Rev. Lett. **56**, 2521 (1986).
  - [10] H. De Raedt and A. Lagendijk, Phys. Rev. Lett. **46**, 77 (1981); H. De Raedt and M. Frick, Phys. Rep. **231**, 107 (1993).
  - [11] A. C. Hewson, *The Kondo Problem to Heavy Fermions* (Cambridge Univ. Press, Cambridge, 1993).
  - [12] A. I. Lichtenstein *et al*, Phys. Rev. Lett. **87**, 067205 (2001).
  - [13] G. D. Mahan, *Many-Particle Physics* (Plenum, N. Y., 1993).
  - [14] T. Maier *et al*, Rev. Mod. Phys. **77**, 1027 (2005).
  - [15] A. I. Lichtenstein and M. I. Katsnelson, Phys. Rev. B **62**, 9283(R) (2000).
  - [16] V. Yu. Irkhin *et al*, Phys. Rev. B **64**, 165107 (2001), Phys. Rev. Lett. **89** 076401 (2002).
  - [17] J. Schäfer *et al*, Phys. Rev. B **72**, 155115 (2005).
  - [18] G. Kotliar *et al*, Phys. Rev. Lett. **87** 186401 (2001).
  - [19] M. Potthoff *et al*, Phys. Rev. Lett. **91**, 206402 (2003).
  - [20] V.V. Mazurenko *et al*, Phys. Rev. B **66**, 081104(R) (2002).
  - [21] A. I. Poteryaev *et al*, Phys. Rev. Lett. **93**, 086401 (2004).
  - [22] S. Biermann *et al*, Phys. Rev. Lett. **94** 026404 (2005).
  - [23] A. Toshi *et al.*, Phys. Rev. B **75**, 045118 (2007).
  - [24] H. Kusunosa, cond-mat/0602451.
  - [25] Of course, the Bethe-Salpeter equation itself is exact irrespective of the value of  $U$ , up to atomic limit. However, the first step of the procedure produces an approximate vertex  $\Gamma$ , which is insufficient in the case of large  $U$ .
  - [26] J. M. Luttinger and J. C. Ward, Phys. Rev. **118**, 1417 (1960).

- [27] G. Baym and L. P. Kadanoff, Phys. Rev. **124**, 287 (1961).
- [28] N. E. Bickers and D. J. Scalapino, Ann. Phys. (N.Y.) **193**, 206 (1989).
- [29] N. D. Mermin and H. Wagner, Phys. Rev. Lett. **17**, 1133 (1966).
- [30] A. N. Rubtsov *et al*, Phys. Rev. B **72**, 035122 (2005).